

J80-152

Electron Collection by Blunt Probes in the Lower Ionosphere

20011
30005

T. M. York,* C.-I. Wu,† and T.W.-K. Lai‡
The Pennsylvania State University, University Park, Pa.

In order to determine electron densities from I - V (current-voltage) data, an analysis of electron collection processes in the weakly ionized, high-pressure ionosphere plasma between 40 and 80 km has been carried out. The diffusion layer concept of ion collection is not applicable. At collector voltages above those for Langmuir saturation, an approximate continuum solution to the electron flux determination is based on experimental values of drift velocity vs E/P . Correction for larger λ_{en} at higher altitudes is included. Electron flux is found to be determined at distances far from the collector, and flow effects are found to be minimal. Electron densities from blunt probe data are compared with those taken simultaneously with other instruments.

Nomenclature

\bar{C}_e	= average random thermal speed of electrons
d	= x position of electric field line
D	= diffusion coefficient
e	= electron charge
E	= electric field intensity
I	= probe current
J	= probe current density
k	= Boltzmann's constant
L	= probe dimension (diameter)
n_e	= electron number density
p	= pressure
R_p	= probe radius
T_e	= electron temperature
U	= probe flight velocity
V	= potential
λ_D	= Debye length
λ_{en}	= electron-neutral mean free path
μ	= mobility
σ	= conductivity

Subscripts

c	= outer edge of diffusion layer
e	= electron
w	= wall (probe)
$+$	= + ion
$-$	= - ion
col	= collection surface

I. Introduction

THE composition and structure of the stratosphere and mesosphere presently are the subject of considerable interest and some controversy.^{1,2} The region between 30 and 100 km is partly the D region of the lower ionosphere and has been termed the middle atmosphere. Specifically, knowledge of the density of free electrons in this region is important in determining electromagnetic transmission

characteristics, as well as in providing clues to the complicated chemistry which includes O_3 and NO_x .^{3,4}

Over a period of years, this region of the upper atmosphere has been probed with Earth-based electromagnetic transmitters as well as with in situ diagnostic devices which are rocket borne.^{5,6} When data relating to electron density are compared, there are evident differences.^{5,7,8} However, there does seem to be a reasonable agreement of data for altitudes above 70 km, where electromagnetic wave techniques are valid. It is at altitudes below 70 km where considerable differences in interpretation remain to be reconciled. The natural reasons for the difficulties are related to the high pressure (0.1 Torr) and low-electron density ($< 10^3 \text{ cm}^{-3}$). It is in this region of the ionosphere where rocket-borne techniques still function, and there is a considerable backlog of data that has been compiled over the years from different diagnostics. Specifically then, this work will examine one technique that has been used to gather ion and electron conductivity and current data in this region of the upper atmosphere; that is, particle collection by biased collectors on rocket-borne probes. Analysis of conductivity and current data is intended to generate electron density information. Accepting the fact that data have generally been gathered with highly biased collectors ($V_w > kT_e/e$), efforts are primarily directed toward understanding this regime of probe operation.

Review of Previous Work

With comprehensive general reviews of electric probes already available in the literature,⁹ as well as review articles dealing specifically with electric probes in high-pressure gases,¹⁰ only a limited discussion of the unique aspects of the problem at hand will be presented. The collection of ion currents in the ionosphere plasma of interest here is collisional, but the collection of saturation electron currents is collisional and transitional. Accordingly, the description of works which relate to these specific plasmas will be presented. Among the earlier papers of note, Su and Lam¹¹ examined the continuum collection of particles by a negative probe of spherical shape in a quiescent plasma. In general, probe radius was considered large compared to the Debye length, but some cases of $R_p \sim \lambda_D$ were evaluated. That work was followed by an analysis¹² of particle collection by an arbitrary shaped body in a flowing plasma. Collision mean free paths were taken to be shorter than sheath thickness; sheath thickness was smaller than the viscous flow boundary layer; and the drift velocities due to any applied fields were taken to be much smaller than thermal velocities. As a part of a program to develop ionosphere diagnostics, Hault¹³ followed the techniques of Lam and solved for the ion current collected in the strong field limit ($V_w > kT/e$), where there was no sheath formation ($\nabla^2 V = 0$); this approach neglected convection by establishing that ion collection occurred within a

Presented as Paper 79-1541 at the AIAA 12th Fluid and Plasma Dynamics Conference, Williamsburg, Va., July 23-25, 1979; submitted Sept. 14, 1979; revision received Dec. 5, 1979. Copyright © American Institute of Aeronautics and Astronautics, Inc., 1979. All rights reserved. Reprints of this article may be ordered from AIAA Special Publications, 1290 Avenue of the Americas, New York, N.Y. 10104. Order by Article No. at top of page. Member price \$2.00 each, nonmember, \$3.00 each. Remittance must accompany order.

Index categories: Atmospheric and Space Sciences; Plasma Dynamics and MHD.

*Professor, Aerospace Engineering Dept. and The Ionosphere Research Laboratory. Member AIAA.

†Graduate Assistant, Nuclear Engineering Dept. and The Ionosphere Research Laboratory.

‡Graduate Assistant, Aerospace Engineering Dept. and The Ionosphere Research Laboratory.

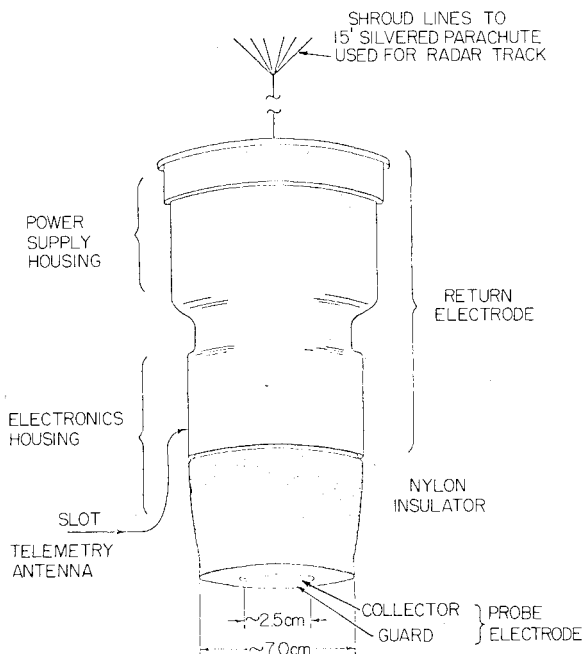


Fig. 1 Parachute-borne blunt probe (Arcas rocket version).

Table 1 Dimensionless parameters and various length scales in the middle atmosphere

Altitude, h	80 km	50 km
Mach number, M	0.3	0.3
Viscous Reynolds number, R_e	10	500
Electrical Reynolds number (ion), Rd_i	10	1000
Viscous boundary layer thickness, δ_{BL}	3.16 cm	0.45 cm
Electric boundary layer thickness (ion), δ_{EBL}	3.16 cm	0.316 cm
Debye length, λ_D	3 cm	12 cm
Electron-neutral mean free path, λ_{en}	20 cm	0.32 cm
Ion-neutral mean free path, λ_{in}	1.6 cm	0.0067 cm

thin surface layer well within the boundary layer. Sonin¹⁴ retained the flow component and carried out a compatible solution; these results agreed with Hoult's at high field strength.

The above-mentioned works were primarily directed toward analyzing ion collection, particularly because of the assumptions that were made. More recently, there has been the publication of several works which specifically address electron collection. Peterson¹⁵ considered the collection of electrons by a positively biased cylindrical probe, as the collection of ions in the turbulent plasma of interest was noted to be velocity dependent even in the collisionless limit. This approximate solution extended the formulation of Talbot and Chou¹⁶ for collection in the transition regime (collision effects added to collisionless solution), but this result is not universally applicable. The limit of large Debye length, $R_p \ll \lambda_D$, was included. A more general approach was followed by Chang and Laframboise,¹⁷ who analyzed stationary plasma with probe size much smaller than the Debye length. The specialized solution for a sphere was shown to be the general form for all shapes. Extensions of a collisional solution to include nonzero collision mean free path were included. However, while the orbit-motion-limited (OML) current for collisionless plasma was reiterated as being correct, it was recognized that the OML solution was exceeded for some limiting cases of their collisional solution at finite λ .

Before discussing the details of analysis in the present work, it will be noted that there are several difficulties in applying

the preceding theories to the diagnostic of interest: 1) because the fields applied are so high, the drift velocities of electrons are on the order of the thermal velocities; therefore, the Einstein relation of mobility to diffusion ($\mu = eD/kT$), which is common in all of the above analyses, is not accurate; 2) because the electron mean free path is large (much larger than the ion mean free path), the notion of a coupled diffusion-mobility solution is not realistic, especially since the mean free path is larger than the thickness of the layer near the surface of collector where diffusion would be dominant; and 3) since the electron collection occurs in air, which is primarily nitrogen, when the drift velocity vs E/p variation for nitrogen is examined, nonlinear behavior is evident and this requires that the actual drift velocity data be used in constructing solutions rather than any simple functional form.¹⁸

II. Equations and Parameters of Particle Collection

Characteristic Parameters of Ionosphere Particle Collection

An illustration of the probe system is shown in Fig. 1. The probe collector element is an aluminum disk in the center of a forward-facing biased electrode composed of collector and guard ring at the end of a cylindrical payload housing. The payload is suspended from a parachute such that the collector faces downward into the flow. The central portion of the electrode, where the electric field is relatively uniform and calculable, is used as a collector and is held at the same potential as the rest of the electrode, which then serves as a "guard" electrode. The electrode is separated by an insulator, usually nylon, from the rest of the payload housing, which is copper or aluminum and serves as a return electrode. A linearly swept potential is applied between the disk and return electrodes. This potential is typically a flat sawtooth on the order of ± 5 to ± 10 V. The division of this applied potential between the probe and return electrode can be calculated^{19,20} and, generally, almost all of the potential appears on the probe electrode, particularly in the daytime when photoelectrons from the return electrode tend to lock the potential of the return electrode to that of the surrounding atmosphere. The slopes of I (current) vs V (voltage) as a function of time are related to dI/dV , and then, using a geometrical shape factor, the current voltage slope is related to the conductivity of the surrounding atmosphere. When the disk is negative, positive conductivities (σ_+) are indicated; when the disk is positive, negative conductivities (σ_-) are indicated. Linear slopes are observed for both σ_+ and σ_- ; at night, when there are generally no electrons present, $\sigma_+, -$ are thought to be good measures of the actual charged particle conductivities of positive and negative ions. In the daytime, above about 40 km, the negative conductivities greatly exceed the positive; hence, σ_- is thought to be due to free electrons. The relatively linear V - I characteristic, which indicates a mobility-like collection mechanism, has led to attempts to derive electron densities,¹³ but at present no precise and tested theory for doing this is known.

Several key parameters take on unique orderings during a data collection event. Since the probe is moving at speeds that are typically 100 m/s, the magnitudes of several flow-related collection parameters are now presented, along with plasma and gas parameters. It will be noted that the electrical Reynolds number, $Rd = ULD^{-1}$ is a measure of the ratio of flow to diffusion effects, and the electric boundary-layer thickness, $\delta_{EBL} = L(RD)^{-1/2}$, indicates the thickness of the region in which mobility and diffusion are significant. The Debye length, $\lambda_D = (kTe)^{1/2} (4\pi n_e e^2)^{-1/2}$, is the order of magnitude of a sheath thickness. Typical values are presented below in Table 1; it should be noted that Rd and δ_{EBL} are for ions (electron values are altered by factors of 10^{-3} and 10^{+3} , respectively).

It should be noted that, for ions, it is valid to treat the collection as collisional. However, the ordering of the thickness of layers must be re-examined for electron collection.

Order-of-Magnitude Analysis of Ion Collection Equations

The governing equations for ion collection for a probe in a flow with velocity U in the continuum limit, and assuming an Einstein relationship, can be written in dimensionless form, as¹²

$$Rd\bar{q} \cdot \nabla n_+ - \nabla n_+ \cdot \nabla \phi - \nabla^2 n_+ = 0 \quad (1)$$

where

$$Rd = \frac{UL}{D_+}, \quad \bar{q} = \frac{\bar{q}}{U}, \quad \nabla = L \bar{\nabla}, \quad n_+ = \frac{\bar{n}_+}{n_{e\infty}}, \quad \phi = \frac{eV}{KT_e} \quad (2)$$

and \bar{q} is flow velocity, L is length scale (probe diameter), \bar{n} is the number density, $n_{e\infty}$ is undisturbed electron number density, V_w is probe voltage, and D_+ is ion diffusion coefficient. The boundary conditions on charge density and potential are:

$$\begin{aligned} n_+(\infty) &= 1 + \alpha & n_+(0) &= 0 \\ n_-(\infty) &= \alpha & n_-(0) &= 0 \\ n_e(\infty) &= 1 & n_e(0) &= 0 \\ \phi(\infty) &= 0 & \phi(0) &= \phi_w \end{aligned}$$

Now, in the D region, $Rd \gg 1$, so the ion density is unperturbed outside the electric boundary layer, and mobility and diffusion processes can be neglected there.

Near the collector surface, however, the situation changes. The boundary condition of zero density at the wall requires a large ion density gradient very near the wall. This region is investigated by stretching the normal coordinate with a dimensionless length scale δ_l . Let $y = \bar{y}\delta_l$ and assume $\delta_l \ll 1$, and in terms of coordinates with y normal to a surface and x along a surface, get

$$\begin{aligned} Rd \left(u \frac{\partial n_+}{\partial x} + v \frac{\partial n_+}{\partial y} \right) + \left(\frac{\partial \phi}{\partial x} \frac{\partial n_+}{\partial x} + \frac{1}{\delta_l^2} \frac{\partial \phi}{\partial \bar{y}} \frac{\partial n_+}{\partial \bar{y}} \right) \\ - \left(\frac{\partial^2 n_+}{\partial x^2} + \frac{1}{\delta_l^2} \frac{\partial^2 n_+}{\partial \bar{y}^2} \right) = 0 \end{aligned} \quad (3)$$

The y convection term is not scaled because it is of unity order. To balance convection with the highest derivative (diffusion) term requires that

$$\delta_l = (Rd)^{-1/2}$$

which is the dimensionless electric boundary-layer thickness. Neglecting terms of order $(Rd)^{-1/2}$

$$\left(u \frac{\partial n_+}{\partial x} + v \frac{\partial n_+}{\partial y} \right) + \frac{\partial \phi}{\partial \bar{y}} \frac{\partial n_+}{\partial \bar{y}} - \frac{\partial^2 n_+}{\partial \bar{y}^2} = 0$$

with boundary condition:

$$n_+(\infty) = 1 + \alpha, \quad n_+(0) = 0$$

This equation is valid inside the electric boundary layer, and $y \rightarrow \infty$ corresponds to the edge of the electric boundary layer. With a thin electric boundary layer, we can write²¹ for the electric field at the wall

$$E_w = -\frac{2V_w}{\pi a}, \quad r \ll a \quad (4)$$

where r is the radial distance from the center of the collector disk to any point in the field, a is the radius of the guard ring, and V_w is the wall or collector potential.

The current density to the collector disk can be expressed

$$J_+ = (n_+ e v_+)_{y=0} \quad (5)$$

where $v_+ = D \nabla n_+ / n_+ - \mu E$, and μ is the ion mobility. These equations were solved by Sonin¹⁴; the result for strong fields with the assumption of an Einstein relation is:

$$J_+ = +en_+ \mu E_w \quad (6)$$

The preceding analysis was carried out assuming flow effects to be significant. An approximate analysis of the same basic equations, but neglecting flow, had been reported by Hoult.¹³ In that work, with the flow assumed incompressible, $\nabla \cdot \bar{q} = 0$; using $\partial \phi / \partial y = -\phi_w f$, where f can be determined from the field profiles of the probe shape, get

$$n_+ = (1 + \alpha) \{1 - \exp f \phi_w y\} \quad (7)$$

With current expressed as

$$dI_+ = eD \left(\frac{\partial n_+}{\partial y} \right)_{y=0} dA_w \quad (8)$$

the result stated in Eq. (6) is again achieved. The characteristic nature of this solution involves collection by diffusion which is dominant in a layer ϕ_w^{-1} thick.

Order-of-Magnitude Analysis of Electron Collection Equations

For a positively biased probe moving with velocity U , the electron conservation equation in a continuum medium is:

$$\beta Rd \bar{q} \cdot \nabla n_e - \nabla \cdot (\nabla n_e - \phi_w n_e \nabla \rho) = 0 \quad (9)$$

where

$$\beta = \left(\frac{D_i}{D_e} \right) \equiv \left(\frac{m_e}{m_i} \right)^{1/2} \ll 1, \quad \rho = \phi / \phi_w$$

with

$$n_e(\infty) = 1, \quad n_e(0) = 0$$

The presence of the term $\beta Rd = ULD_e^{-1}$ makes analysis of electron collection different. The specification that $\beta Rd \ll \phi_w$

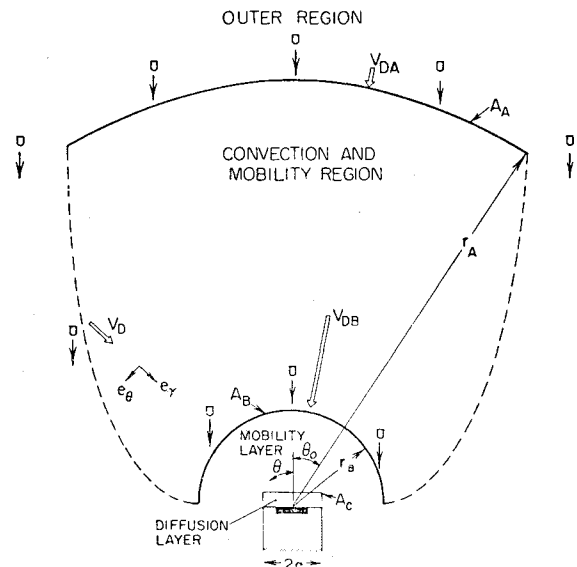


Fig. 2 General structure of regions for approximate model of electron collection with flow.

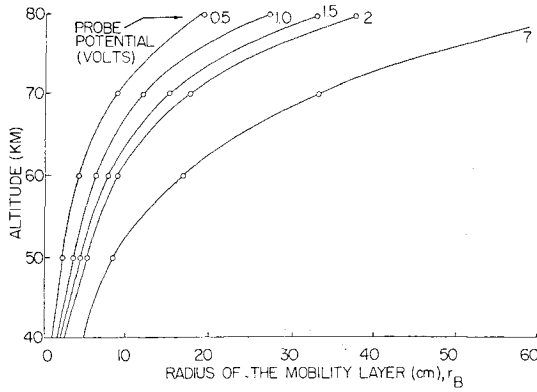


Fig. 3 Influence of altitude on the mobility layer radius r_B with varying probe potential.

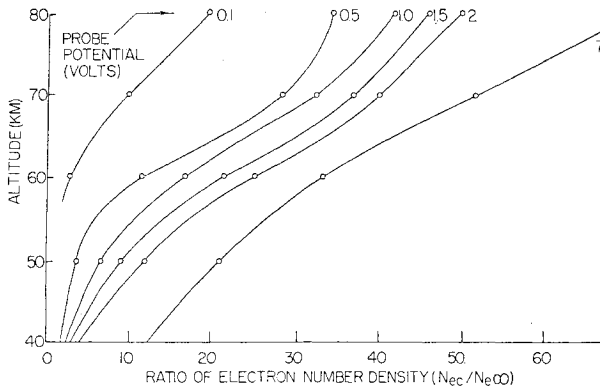


Fig. 4 Influence of altitude on $n_{ec}/n_{e\infty}$ with varying probe potential.

implies that convection is only a weak influence, and as ϕ_w is the largest parameter in Eq. (9) immediately implies that mobility term $\nabla n_e \cdot \nabla \rho$ will be dominant in electron collection. An electron moving at a distance approximately L away from the probe will be governed by mobility. For distances nearer or farther away, layers of different thickness are relevant.

For distances close to the collector, the scaling of mechanisms can be understood as follows. From the preceding,

$$\frac{\beta R d}{\phi_w} \left(u \frac{\partial n_e}{\partial x} + v \frac{\partial n_e}{\partial y} \right) + \left(\frac{\partial n_e}{\partial x} \frac{\partial \rho}{\partial x} + \frac{\partial n_e}{\partial y} \frac{\partial \rho}{\partial y} \right) - \frac{1}{\phi_w} \left(\frac{\partial^2 n_e}{\partial x^2} + \frac{\partial^2 n_e}{\partial y^2} \right) = 0 \quad (10)$$

With the parameter ϕ_w^{-1} , as a coefficient of the last term, a boundary-layer behavior of electron density near the probe is indicated. Letting $y = \eta \delta_2$, with $\delta_2 \ll 1$

$$\begin{aligned} \frac{\partial^2 n_e}{\partial \eta^2} &+ \delta_2 \frac{\partial^2 n_e}{\partial x^2} - \phi_w \delta_2 \frac{\partial n_e}{\partial x} \frac{\partial \rho}{\partial x} - \phi_w \delta_2 \frac{\partial n_e}{\partial \eta} \frac{\partial \rho}{\partial y} \\ (A) & \quad (B) \quad (C) \\ -\beta R d \delta_2^2 \left(u \frac{\partial n_e}{\partial x} + v \frac{\partial n_e}{\partial \eta} \right) &= 0 \quad (D) \end{aligned} \quad (11)$$

Note that $\partial \rho / \partial y$ is not scaled, as potential decreases slowly and boundary-layer behavior is not possible. To analyze this equation near the collector, the mobility term (C) is used to balance the diffusion term (A). This results in $\delta_2 = 1/\phi_w$ —again a diffusion layer thickness—and the

dominant terms for particle collection near the surface become

$$\frac{\partial^2 n_e}{\partial \eta^2} - \frac{\partial n_e}{\partial \eta} \frac{\partial \rho}{\partial y} = 0 \quad (12)$$

with $n_e(\infty) = n_{ec}$, where c is the condition at edge of diffusion layer; $n_e(0) = 0$. In a thin layer, the electric field can be treated as constant, so

$$n_e = n_{ec} \left[1 - \exp \left(\frac{\partial \rho}{\partial y} \eta \right) \right] \quad (13)$$

This approach is distinctly different in the use of n_{ec} , since other works assume $n_{e\infty}$ for η large.

For distances that are large compared to body dimension, both spatial variables can be scaled to establish orders of magnitude of effects. When a scaling with $\bar{x} = x/\delta_3$, $\bar{y} = y/\delta_3$ is used, $\delta_3 \ll 1$, and convection and mobility terms are balanced,

$$\delta_3 = \phi_w / (\beta R d) \quad (14)$$

This represents the extent of an intermediate layer where both convection and mobility are active.

Accordingly, for electron collection with flow, four regions can be identified; in dimensionless variables:

- 1) $0 < y < \phi_w^{-1} = \delta_2$ diffusion-mobility dominant region
- 2) $\phi_w^{-1} < y < 1 = \delta_1$ mobility dominant region
- 3) $1 < y < \phi_w / \beta R d = \delta_3$ mobility-convection dominant region
- 4) $\phi_w / \beta R d < y$ convection dominant region

Estimation of Electron Collection Parameters with Flowing Plasma

Solution of Eq. (10) is difficult because the perturbed regions for electrons extend far from the probe and it has been seen that different mechanisms dominate at different distances. A simple, approximate solution will be outlined later, but prior to that, it is useful to categorize changes that occur in electron density during the collection process, as well as other parameters such as collection trajectories.

Presuming that the continuum concept of a diffusion layer is valid, the current to the probe can be expressed

$$I_e = e D_e \left(\frac{\partial n_e}{\partial y} \right)_{y=0} A_{col} \quad (15)$$

and using Eq. (13)

$$I_e = -e n_{ec} D_e \left(\frac{\partial \phi}{\partial y} \right)_{y=0} A_{col} \quad (16)$$

and for a thin diffusion layer

$$I_e = e n_{ec} D_e \left(\frac{2 V_w}{\pi a} \right) A_{col}$$

where n_{ec} is the electron density at the edge of the diffusion layer. The general geometry being discussed is shown in Fig. 2. Considering Fig. 2, in the mobility layer, electron dynamics are determined by the electric field and the electric field at the outer extent of this region can be expressed as

$$E_B = -(2a V_w / \pi r_B^2) \quad r_B \gg a \quad (17)$$

where r_B is the location of the outer radius of the mobility region and its value is unknown. In view of the fact that

convection is neglected in the mobility layer, the outer location of the mobility layer will be evaluated through an ad hoc assumption that $v_{DB} \approx 10 U$, where U is rocket velocity. Knowing altitude and probe voltage V_w , and using experimental values of v_D vs E/p , r_B can be determined. Particle flux conservation will be used to relate n_{ec} to n_{eB} as

$$n_{eB}(A_B v_{DB} + \pi r_B^2 U) = n_{ec}(A_c v_{Dc} + \pi a^2 U) \quad (18)$$

A region farther from the probe surface will evidence weaker drift velocities and stronger flow effects; this is referred to as the convection and mobility region, Fig. 2. In order to define the outer surface of this region, an ad hoc assumption is made again that it occurs at $v_{DA} = 0.1 U$. For specified velocity, the location of the surface r_B can be determined from v_D vs E/p data for nitrogen. Two specific calculations were carried out to categorize this region. First, with flow and drift velocity data, the trajectories of electrons were analyzed to determine the lateral extent of the collection surface at A within which all electrons would be collected by the disk or guard ring. In Fig. 2, this lateral extent is indicated by the angle θ_0 for the radius r_A . Knowing r_A , r_B , and the v_D variation, θ_0 was numerically solved; the drift velocity inside this region was expressed as²² (see Fig. 5, below)

$$v_D = 10^{(\log_{10} E/p + 7.065)} \quad (19)$$

Taking typical launch data, it was found that $\theta_0 = 28$ deg was the value that resulted over altitudes from 40-80 km. Second, with this identification of lateral extent, and presuming the flux of $Un_{e\infty}A_A$ at r_A ($n_{eA} \approx n_{e\infty}$), flux conservation allows the calculation of n_{eB}/n_{eA} , n_{ec}/n_{eB} . Interestingly, it was found that $n_{eB}/n_{e\infty} = 1$, so there is no perturbation of electron density until closer to the surface. Values of the radius where mobility becomes dominant are shown in Fig. 3. Particle flux conservation also allowed calculation of the ratio $n_{ec}/n_{e\infty}$; this is presented in Fig. 4. It can be seen that there is an expected increase in electron density near the probe surface.

It will be noted that the above discussion in this section is not intended to indicate an acceptable analysis of electron collection, but only to establish orders of magnitude of effects and phenomenology. An approximate analysis using the same physical concepts will now be presented.

III. Development of Analysis of Electron Collection

Approximate Analysis of Electron Collection by Blunt Probes in Ionosphere Plasmas

Based on the description of physical behavior outlined earlier, an approximate analysis of electron collection by blunt probes will now be outlined. In basic terms, the dimensional equation for electron species conservation is written

$$\vec{q} \cdot \nabla n_e + \nabla \cdot (-D_e \nabla n_e + \mu_e n_e \nabla V) = 0 \quad (20)$$

$$\nabla^2 V = 0 \quad (21)$$

with boundary conditions:

$$r=0: \quad n_+ = 0 \quad n_e = 0 \quad V = V_w$$

$$r=\infty: \quad n_+ = n_{+\infty} \quad n_e = n_{e\infty} \quad V = 0$$

The electric field can be determined independently of the particles.

With the electric field pattern and magnitudes determined, the value of electron drift velocity in air at any point in the field will be approximated by drift velocity data in nitrogen published by McDaniel.²² This variation is shown in Fig. 5. The very interesting character of this graph is that there is a definite plateau or constant value drift velocity while E/p

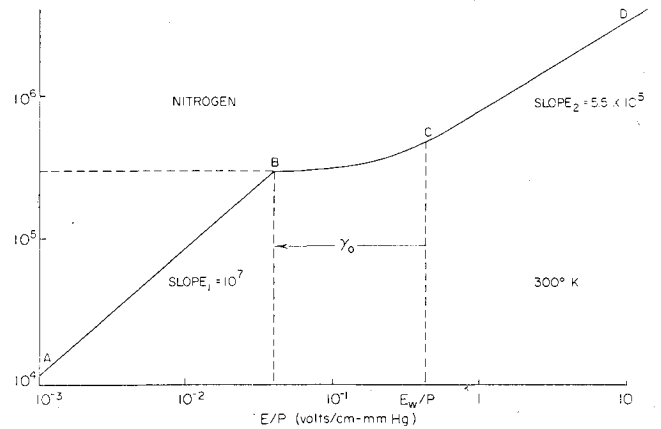


Fig. 5 Experimental data on the drift velocity of electrons in nitrogen (Fig. 11-3-11 D of Ref. 22).

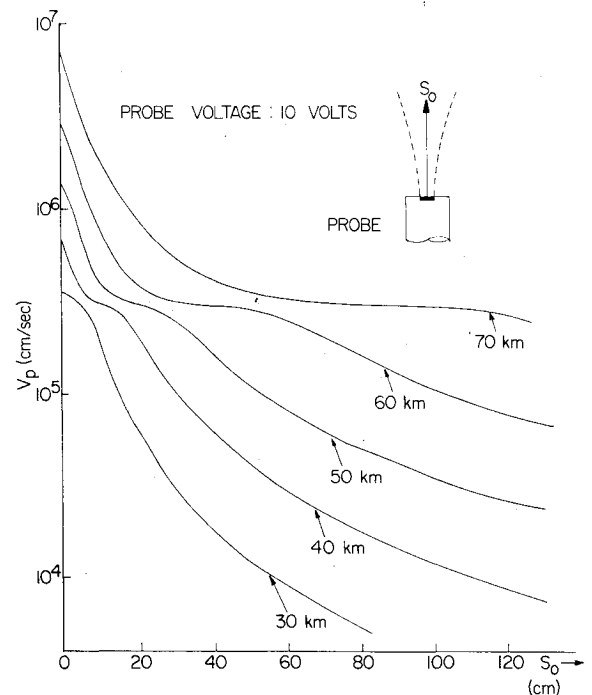


Fig. 6 The drift velocity vs S_0 for different altitudes.

values decrease over an order of magnitude. A typical value for E_w/p is shown in the figure, with corresponding drift velocity about 5×10^5 cm/s. Clearly, then, the drift velocity is on the same order as random thermal velocity $v_D \approx v_{th}$, which means that there will be inelastic electron collisions with heavy particles and the standard assumption of an Einstein relation should not be used. Also, it can be seen that $v_D \gg v_{flow}$; therefore, flow effects should be negligible. Both of these variations will be more fully described for typical flight conditions.

Regarding the diffusion term in the species conservation equation, as has been noted above, diffusion will be a significant effect only in the thin diffusion layer near the surface. The thickness of this layer was shown to be $\delta_D \approx L\phi_w^{-1}$, when collisional effects are dominant. However, when consideration is given to the middle atmosphere plasma, the electron-neutral mean free path can be expressed as²³

$$\lambda_{en}(\text{cm}) = \bar{C}_e / 8.4 \times 10^7 p \quad (22)$$

where p is the neutral gas density (mm Hg) and \bar{C}_e is the thermal velocity of the electrons (cm s^{-1}). Since $\lambda_{en} > L\phi_w^{-1}$, the diffusion layer concept is not appropriate to describe near-

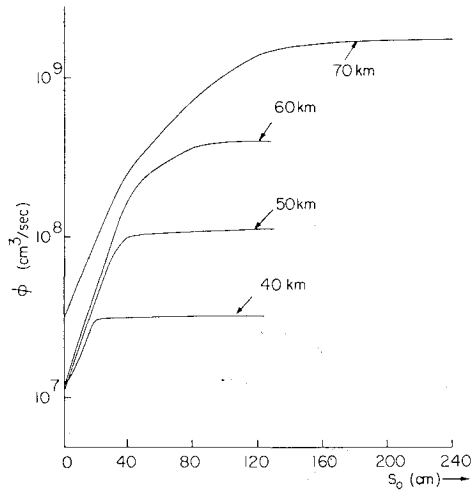


Fig. 7 Electron flow, ϕ , as a function of distance from collector (10 V) for different altitudes.

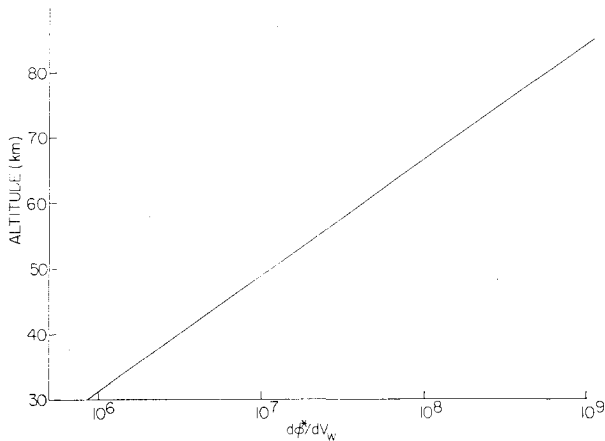


Fig. 8 Derivative of saturated electron flow with respect to probe voltage as a function of altitude.

surface particle collection. Rather, a model of random thermal flux is more appropriate, and it will be developed below.

With the preceding specifications of electron collection conditions, the species conservation equation takes the simple form

$$\nabla \cdot (\mu_e n_e \nabla V) = 0 \quad (23)$$

or

$$\oint_A (\mu_e n_e E) \cdot n dA = 0 \quad (24)$$

To solve for electron collection, E flux generated by the electric field of the collection disk and guard ring surfaces must be determined. It will be assumed that particle flux within electric field lines will be conserved. Based on the experimental variation of v_D vs E/p , a simple analytical model can be developed.

The flux of electric field lines can be expressed through Gauss' law by

$$AE = c_I (\text{const}) \quad (25)$$

where A and E are local flux tube cross-sectional area and magnitude of the electric field at a y location. Particle flux conservation yields

$$n_e A v_D = C_2 (\text{const}) \quad (26)$$

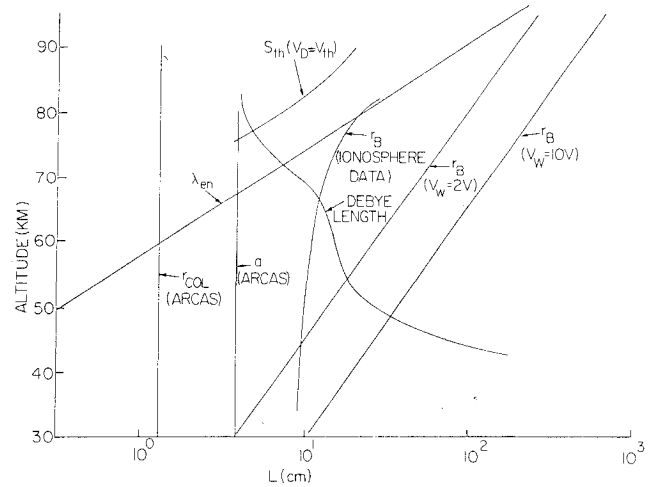


Fig. 9 Variation of characteristic lengths for electron collection as a function of altitude.

so

$$n_e v_D E^{-1} = C_3 (\text{const}) \quad (27)$$

or

$$n_e v_D (E/p)^{-1} = C_4 (\text{const}) \quad (28)$$

From this equation, it can be argued that in regions where the slope $v_D (E/p)^{-1}$ is constant, then density should be a constant. Accordingly, on Fig. 5, at great distances away from the probe or small E/p , $n_e = n_{e\infty}$, and it will be constant up to a distance compatible with E/p at B. As the electron flux moves toward the surface, n_e will change. Considering the region C-B on the figure, with collector conditions near C, as we increase the distance away from the probe, the area of the flux tube increases, drift velocity decreases, and the maximum particle flux would occur at point B, where $v_{DB} = 3 \times 10^5$ cm/s and $E_B/p = 4 \times 10^{-2}$ V cm⁻¹ mm Hg⁻¹. With Eqs. (4) and (17), at B we have

$$(E/p)_B = (E_w/p) a^2 / r_B^2 \quad (29)$$

so

$$r_B = 5a (E_w/p)^{1/2} \quad (30)$$

with Eq. (25)

$$A_B = \pi r_{\text{col}}^2 r_B^2 / a^2 = 25 \pi r_{\text{col}}^2 (E_w/p)$$

Accordingly, if all particles collected at position r_B move in an electric flux tube toward the collector disk,

$$I_e = e v_{DB} n_{e\infty} A_B \quad (31)$$

With the preceding equations, this can be substituted into and rearranged to give

$$I_e = 25 \cdot e \cdot v_{DB} n_{e\infty} A_{\text{col}} (E_w/p) \quad (32)$$

or

$$I_e = 50 \cdot e \cdot \frac{r_{\text{col}}^2}{a} \cdot v_{DB} \cdot \frac{n_{e\infty} V_w}{p} \quad (33)$$

so

$$n_{e\infty} = I_e \left\{ 50 \cdot e \cdot \frac{r_{\text{col}}^2}{a} \cdot \frac{v_{DB} \cdot V_w}{p} \right\}^{-1} \quad (34)$$

Alternatively, it is standard fashion to use conductivity values as

$$\frac{dI_e}{dV_w} = \frac{2r_{\text{col}}^2}{a} \sigma_- \quad (35)$$

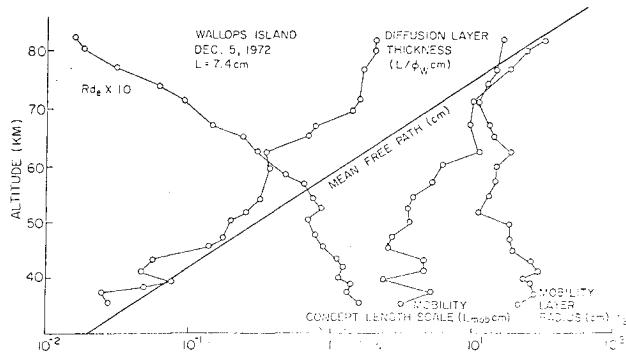


Fig. 10 Variation of length scales for electron collection as a function of altitude.

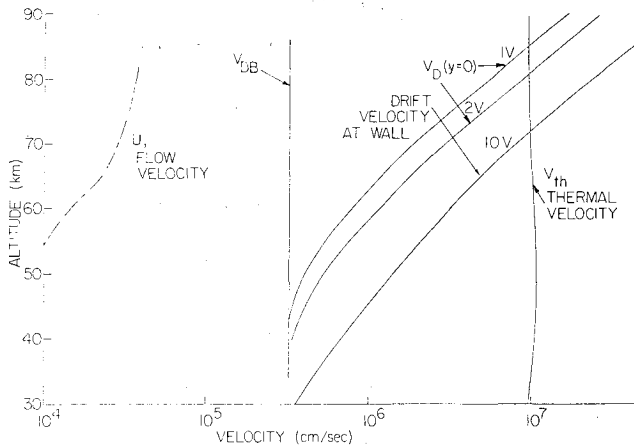


Fig. 11 Variation of characteristic velocities of electron collection as a function of altitude.

then

$$n_{e\infty} = (50 \cdot e \cdot v_{DB}) p \sigma_- \quad (36)$$

and

$$n_{e\infty} (\text{cm}^{-3}) = 8.35 \times 10^{11} p (\text{mm Hg}) \sigma_- \left(\frac{\text{mho}}{\text{cm}} \right), \lambda_{en} \ll a$$

This simple formula includes all the basic ideas for determination of electron density from conductivity, but several points must be noted. First, this equation presumes that the electric field flux tube to the collector disk gathers all particles (i.e., $\lambda_{en} \ll a$); it makes no accommodation for longer mean free path effects. Second, there is the presumption that maximum flux is generated at point B, but this has not been proven. Rather than turn to an analytical formulation, which can be done, physical behavior of flux with specific probes and voltages will be examined.

Considering the drift velocity and flux behavior, specific variations are shown for a Super Arcas type probe ($r_{\text{col}} = 1.30$ cm, $a = 3.65$ cm) in Figs. 6 and 7. It can be seen that very definite limiting values of drift velocity and flow, $\phi = v_D A$ can be identified graphically; these values do correspond to the saturation of flux at r_B from velocity v_{DB} and A_B , and confirms the procedure.

Considering the mean free path effects which should be accounted for at higher altitudes, the basic idea can be visualized in Fig. 2. In this figure, the idea is that saturation flux will again be determined at condition (state) B, radius r_B , and field lines will draw all particles to the surface of disk and guard ring. However, since mean free path effects on this scale can result in rearrangement of electrons between guard ring and disk, the following approximate analysis is carried

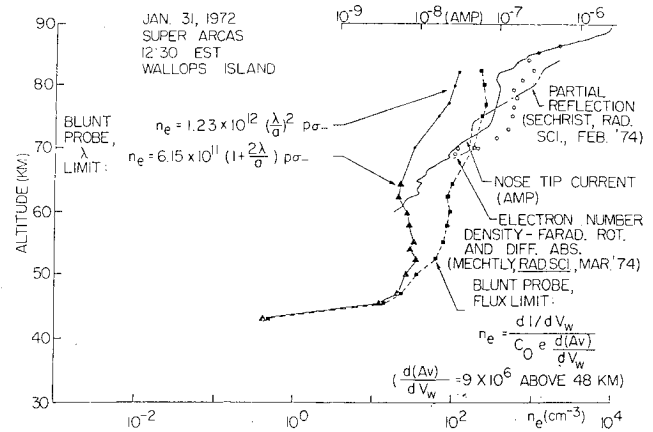


Fig. 12 Electron density from blunt probe data compared with reference diagnostics, Jan. 31, 1972.

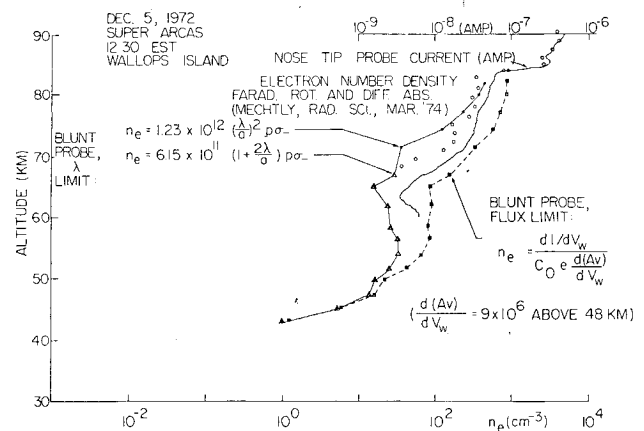


Fig. 13 Electron density from blunt probe data compared with reference diagnostics, Dec. 5, 1972.

out. First, particle flux conservation between B at r_B and the surface can be written

$$n_{e\infty} K^{-1} A_0 v_{DB} = n_{e\lambda} [\pi a^2 + 2\pi a \lambda_{en}] \bar{C}_e / 4 \quad (37)$$

where A_0 is taken as a hemispherical surface area, and K is a factor that indicates the ratio of the area of a hemisphere to the area for the flux tube which meets the outer radius of the guard ring. The idea presented here is that flux lines attract particles to the surface, but particles that reach the collector and guard ring arrive there by local kinetic flux. The preceding equation allows $n_{e\lambda}$ to be determined. Second, the current to the collector disk is expressed as

$$I_e = e \cdot \pi (r_{\text{col}})^2 \cdot n_{e\lambda} \cdot \frac{\bar{C}_e}{4} \quad (38)$$

then

$$I_e = e \cdot \pi (r_{\text{col}})^2 \cdot n_{e\infty} \left[\frac{K^{-1} A_0}{\pi a^2 + 2\pi a \lambda_{en}} \right] v_{DB} \quad (39)$$

and substituting for A_0

$$n_{e\infty} = \left(1 + 2 \frac{\lambda}{a} \right) K (0.4 \times 10^{12}) p \sigma_-, \lambda_{en} \leq a \quad (40)$$

For Loki-Dart rockets ($r_{\text{col}} = 1.27$ cm, $a = 2.0$ cm), $K = 2.14$ and for Super Arcas rockets, $K = 1.54$. In a similar analysis for larger mean free paths,

$$n_{e\infty} = (\lambda_{en}/a)^2 K (0.8 \times 10^{12}) p \sigma_-, \lambda_{en} > a \quad (41)$$

It should be noted that, in the equations, $n_{e\infty}$ can be determined from I_e at V_w data or dI_e/dV_w data. The latter method is preferable because it is not sensitive to any local atmospheric E fields.

Supplementary Notions for Electron Collection at Larger Mean Free Path

The basic fact that has become evident is that as bias voltages applied to the disk and guard ring are increased, the electron flux to the collector will increase. As it has been determined that flux composed of $n_{eB}A_B v_{DB}$ will saturate with $n_{e\infty}$, and since $v_{DB} = \text{constant}$, the variations of flux with voltage are due to A_B changes. Specifically, if

$$I_e \equiv en_{e\infty} \phi^*$$

where ϕ^* is saturated volume flow rate ($v_{DB}A_B$) then

$$\frac{dI_e}{dV_w} = en_{e\infty} \frac{d\phi^*}{dV_w}$$

or

$$n_{e\infty} = \frac{I}{e} \frac{dI_e/dV_w}{d\phi^*/dV_w}$$

The term $d\phi^*/dV_w$ reflects dA_B/dV_w . The variation of $d\phi^*/dV_w$ has been graphed in Fig. 8. It can be seen that there is an exponential increase of $d\phi^*/dV_w$ with altitude. However, with higher altitude and larger λ_{en} , particles can also be lost from the flux tubes in this scheme, and this loss has not been accounted for. An approximate method of including this loss due to larger λ_{en} would be to hold $d\phi^*/dV_w$ constant above an appropriate altitude. Several methods of setting this altitude have been evaluated analytically. Specifically, 65 km is indicated by values of d at A_B being equated to λ_{en} . However, setting the value of $d\phi^*/dV_w$ at a somewhat lower altitude (48 km) does seem to work moderately well. At the present time, such a method is regarded as somewhat arbitrary, and it is considered not well founded for our application. Its use in evaluating data will be presented for comparison purposes only.

IV. Application of Analysis to Rocket-Borne Blunt Probe Data

Orders of Magnitude of Plasma and Probe Parameters for Electron Collection

The orders of magnitude of parameters presented earlier are somewhat general, but on application to ionosphere data, the parameters take on distinct values at different altitudes due to voltages, pressure, etc.

First regarding length scales, for a typical mid-day data record with the Super Arcas probe, the length scales are shown in Fig. 9. It can be seen that saturation distance r_B is quite large for high voltages and high altitudes; yet, for voltages applied in actual data recording, it stays about 10-20 cm. The Debye length is smaller than r_B above 70 km, but is larger below. The λ_{en} is generally smaller than r_B . Other derived length scales are presented in Fig. 10. The parameters there have been defined with the exception of L_{mob} , the mobility length scale. The mobility length scale is related to velocity gain in one λ_{en} , as

$$\frac{\Delta v}{v_{th}} = \frac{\pi}{8} \frac{eV_w}{kT_e} \cdot \frac{\lambda_{en}}{L} \equiv \frac{L_{mob}}{L}$$

When $L_{mob} > L$, the mobility concept is questionable.

Second regarding velocity ordering, values of thermal velocity, drift velocity near probe surface, drift velocity at saturation location, and flow velocity are shown in Fig. 11.

Blunt Probe Data Reduction and Comparison of n_e with Other Diagnostic Indications

The analysis of the electron collection processes outlined earlier resulted in formulas for electron density from $I-V$ data or (dI/dV) data. In order to examine the relevance of these formulas and this analysis, it is useful to compare the predictions of number density with those of other diagnostics.¹⁸ Fortunately, independent sets of data have been taken with blunt probes on days and at times that allow such comparison. First, during the Winter Anomaly campaign at Wallops Island, on two days (Jan. 31, 1972, and Dec. 5, 1972), Hale and Mitchell²⁴ had launched a Super Arcas blunt probe shortly after a probe package had been launched by researchers from the University of Illinois.^{5,7} The latter probe was supersonic and fitted with a nosetip Langmuir probe, as well as electronics appropriate for Faraday rotation and differential absorption measurements. (Comparisons were also made with partial reflection data in some published cases.) Reduction of data taken during each of these events will be presented and discussed. It is to be noted that there will not be a comprehensive evaluation of general techniques, specific equipment limitations, or detailed calculation procedures presented here. These will be presented in another work.²⁵ However, these comparisons are intended to serve as a basis for a relative evaluation of all diagnostics.

The electron density points (Ref. 7) for Jan. 31, 1972 (Fig. 12) are primarily from Faraday rotation measurements; the partial reflection data were taken at Wallops Island at 12:12 local time. It should be noted that the Illinois nosetip density data are not reduced absolutely; they are graphed and then shifted laterally until the curve fits n_e data at one predetermined point. Without attempting detailed description or discussion of these predictions from blunt probe data, the λ_{en} limit analysis is the same order of magnitude, with a similar shape as those indicated by other diagnostics. This was generally an average day during the Winter Anomaly, and the predictions can be concluded to be in reasonable agreement.

The predicted electron number densities for Dec. 5, 1972 are shown in Fig. 13. The electron density points from Mechtly⁷ are primarily differential absorption. Clearly, there is very good agreement here of the blunt probe predictions with all other diagnostics.

It does appear that the analysis presented here should be tested further under ionosphere and laboratory controlled conditions. In fact, scaled laboratory tests have been completed and serve to verify the accuracy of the electron density prediction from the new blunt probe analysis.²⁶

Acknowledgment

This research was carried out under the support of National Science Foundation Grant NSF-ATM-76-81004.

References

- ¹"The Upper Atmosphere and Magnetosphere," The Geophysics Study Committee, National Research Council, National Academy of Science, Washington, D.C., 1977.
- ²Thomas, L., "Recent Developments and Outstanding Problems in the Theory of the D-Region," *Radio Science*, Vol. 9, Feb. 1974, pp. 121-136.
- ³Hoock, D. W. and Heaps, M. G., "DAIRCHEM: A Computer Code to Model Ionization-Deionization Processes and Chemistry in the Middle Atmosphere," Users Manual, Atmospheric Sciences Lab., White Sands Missile Range, N. Mex., March 1978.
- ⁴Heaps, M. G., "The 1970 Solar Eclipse and Validation of D-Region Models," ASL-TR-0002, Atmospheric Sciences Lab., White Sands Missile Range, N. Mex., March 1978.
- ⁵Sechrist, Jr., C. F., "Comparisons of Techniques for Measurement of D-Region Electron Densities," *Radio Science*, Vol. 9, Feb. 1974, pp. 137-149.
- ⁶Mitchell, J. D. and Hale, L. C., "Observation on the Lowest Ionosphere," *Space Research XIII*, Akademie-Verlag, Berlin, 1973, pp. 471-476.
- ⁷Mechtly, E. A., "Accuracy of Rocket Measurements of Lower

Ionosphere Electron Concentration," *Radio Science*, Vol. 9, March 1974, pp. 373-378.

⁸Ferraro, A. J., Lee, H. S., Rowe, J. N., and Mitra, A. P., "An Experimental and Theoretical Study of the D-Region—I," *Journal of Atmospheric and Terrestrial Physics*, Vol. 36, 1974, pp. 741-754.

⁹Chung, P. M., Talbot, L., and Touryan, K. J., *Electric Probes in Stationary and Flowing Plasmas: Theory and Application*, Springer-Verlag, New York, 1975.

¹⁰Smy, P. R., "The Use of Langmuir Probes in the Study of High Pressure Plasmas," *Advances in Physics*, Vol. 25, 1976, pp. 517-553.

¹¹Su, C. H. and Lam, S. H., "Continuum Theory of Spherical Electrostatic Probes," *The Physics of Fluids*, Vol. 6, Oct. 1963, pp. 1479-1491.

¹²Lam, S. H., "A General Theory for the Flow of Weakly Ionized Gases," *AIAA Journal*, Vol. 2, Feb. 1964, pp. 256-262.

¹³Hoult, D. P., "D-Region Probe Theory," *Journal of Geophysical Research*, Vol. 70, July 1965, pp. 3183-3187.

¹⁴Sonin, A. A., "Theory of Ion Collection by a Supersonic Atmospheric Sounding Rocket," *Journal of Geophysical Research*, Vol. 72, Sept. 1967, pp. 4547-4557.

¹⁵Peterson, E. W., "Collisional Effects on the Transient Response of Cylindrical Electrostatic Probe," *Journal of Applied Physics*, Vol. 44, Feb. 1973, pp. 636-643.

¹⁶Talbot, L. and Chou, Y. S., "Langmuir Probe Response in the Transition Regime," in *Rarefied Gas Dynamics*, C. L. Brundin, ed., Academic Press, New York, Vol. 2, 1969, pp. 1723-1737.

¹⁷Chang, J. S. and Laframboise, J. G., "Probe Theory for Arbitrary Shape in a Large Debye Length, Stationary Plasma," *The*

Physics of Fluids, Vol. 19, Jan. 1976, pp. 25-31.

¹⁸York, T. M., "Measurement of Electron Densities in the Middle Atmosphere Using Rocket Borne Blunt Probes," Rept. IRL-IR-67, Ionosphere Research Lab., The Pennsylvania State University, University Park, Pa., Jan. 1979.

¹⁹Hale, L. C., Hoult, D. P., and Baker, D. C., "A Summary of Blunt Probe Theory and Experimental Results," in *Space Research VIII*, North Holland, Amsterdam, 1968.

²⁰Hale, L. C., "Parameters of the Low Ionosphere at Night Deduced from Parachute Borne Blunt Probe Measurements," in *Space Research VII*, North Holland, Amsterdam, 1966.

²¹Jackson, J. D., *Classical Electrodynamics*, John Wiley, New York, 1963.

²²McDaniel, E. W., *Collision Phenomena in Ionized Gases*, John Wiley, New York, 1964.

²³Benson, R. F., "Electron Collision Frequency in the Ionospheric D-Region," *Radio Science*, Vol. 68D, Oct. 1964, pp. 1123-1125.

²⁴Cipriano, J. P., Hale, L. C., and Mitchell, J. D., "Relations Among Two Ionosphere Parameters and A3 Radio Wave Absorption," *Journal of Geophysical Research*, Vol. 79, May 1974, pp. 2260-2265.

²⁵York, T. M., Olsen, R. O., and Mitchell, J. D., "Electron Density Determination in the Middle Atmosphere Using Rocket Borne Blunt Probes," in preparation.

²⁶York, T. M., Brasfield, R., and Kaplan, L. B., "Evaluation of Current Collection by Blunt Electrostatic Probes in a Scaled Lower Ionosphere Laboratory Experiment," AIAA Paper 80-0093, Jan. 1980.

From the AIAA Progress in Astronautics and Aeronautics Series . . .

SPACE-BASED MANUFACTURING FROM NONTERRESTRIAL MATERIALS-v. 57

Editor: Gerard K. O'Neill; Assistant Editor: Brian O'Leary

Ever since the birth of the space age a short two decades ago, one bold concept after another has emerged, reached full development, and gone into practical application—earth satellites for communications, manned rocket voyages to the moon, exploration rockets launched to the far reaches of the solar system, and soon, the Space Shuttle, the key element of a routine space transportation system that will make near-earth space a familiar domain for man's many projects. It seems now that mankind may be ready for another bold concept, the establishment of permanent inhabited space colonies held in position by the forces of the earth, moon, and sun. Some of the most important engineering problems are dealt with in this book in a series of papers derived from a NASA-sponsored study organized by Prof. Gerard K. O'Neill: how to gather material resources from the nearby moon or even from nearby asteroids, how to convert the materials chemically and physically to useful forms, how to construct such gigantic space structures, and necessarily, how to plan and finance so vast a program. It will surely require much more study and much more detailed engineering analysis before the full potential of the idea of permanent space colonies, including space-based manufacturing facilities, can be assessed. This book constitutes a pioneer foray into the subject and should be valuable to those who wish to participate in the serious examination of the proposal.

192 pp., 6 × 9, illus., \$15.00 Mem., \$23.00 List

TO ORDER WRITE: Publications Dept., AIAA, 1290 Avenue of the Americas, New York, N. Y. 10019